Experimental study of heat transfer performance of horizontal-tube falling film evaporator

Qingsheng Li*, Yongze Shen, Shengwang Lai

School of Mechanical and Power Engineering, Nanjing Tech University, Nanjing, Jiangsu 211816, China, Tel. +86 025 58139953; email: lqsh@njtech.edu.cn (Q. Li), Tel. +86 13512500658; email: 804175246@qq.com (Y. Shen), Tel. +86 15651772108; email: 1398248305@qq.com (S. Lai)

ABSTRACT

In this study, an experiment was conducted to analyze the heat transfer performance of a horizontal-tube falling film evaporator. The evaporator performance was tested with water and sodium chloride brine. The heat transfer performance of the crest and column sections for liquid film flow outside the tubes in a columnar flow pattern was investigated. The effects of the flow rate, tube spacing, outer tube diameter, feed temperature, and salinity on the local heat transfer coefficient outside the titanium-made heat exchange tube were studied. According to the findings of this study, (i) the local heat transfer coefficient of the crest section increases with flow rate and feed temperature, decreases with tube spacing and salinity, (ii) the local heat transfer coefficient of the column section increases with an increase in the flow rate, tube spacing, feed temperature, but decreases with salinity, and (iii) the influence of outer tube diameter on the local heat transfer coefficient of the crest and column sections varies with the circumferential angle. However, when $D_2 = 19$ mm, the variation in the local heat transfer coefficient is not consistent with that of other horizontal tubes because of $D_2 < D_1$. In a columnar flow pattern, the crest and column formed by the flow outside the liquid film tube are two important fluctuation areas of the liquid film. In this paper, the local heat transfer coefficient of the crest and column is obtained through the experiment, which provides the foundation for improving the heat transfer performance of the horizontal-tube falling film evaporator.

Keywords: Falling film evaporator; Horizontal tube; Heat transfer coefficient; Crest section; Column section

1. Introduction

The composition and characteristics of industrial wastewater discharged from petrochemical industry are complex. The direct discharge of industrial wastewater seriously polluted to water sources and harms people's health. The production shows that the utilization of multi-effect evaporation technology can realize the recovery of freshwater resources with high efficiency and low energy consumption. Compared with other membrane evaporators, horizontal-tube falling film evaporators have the advantages of high heat transfer coefficient, small temperature difference, less scaling, and full use of low-grade heat source, etc., which have significant energy-saving advantages in the application of multi-effect evaporation process of industrial wastewater [1,2].

Three methods (theoretical analysis, numerical simulation, and experimental verification) are currently employed in studies on factors affecting heat transfer in horizontal-tube falling film evaporators [3–5]. There are certain limitations in the results of these studies owing to the impact of the assumptions in heat transfer calculation

* Corresponding author.

models. In the experimental investigation, scholars primarily conduct research on the heat transfer performance of horizontal tubes from aspects, such as feed temperature, the flow rate, outer tube diameter, salinity, liquid distributor height, and heat flux, but the results are different. Parken et al. [6] studied the heat transfer performance of the horizontal smooth tube, and found that the average heat transfer coefficient increased with the increase of feed temperature and the flow rate, and decreased with the increase of outer tube diameter. The effect of feed temperature on the heat transfer coefficient was studied experimentally when the working fluid was water, Ganic and Roppo [7] discovered that the increase of feed temperature had little effect on the heat transfer coefficient. Hu and Jacobi [8] studied the influence of outer tube diameter on the heat transfer coefficient, and found that the smaller the outer tube diameter is, the larger the proportion of the top impact area formed by the liquid film flow to the whole pipe circumference is, and the area has a higher local heat transfer coefficient, so the small-diameter evaporation pipe has a higher average heat transfer coefficient. When studying the influence of outer tube diameter on the heat transfer coefficient, Xu et al. [9] found that the smaller the outer tube diameter, the more violent the liquid film fluctuation will be, and the higher the average heat transfer coefficient will be. The experimental study was carried out with brine as working fluid, Slesarenko [10,11] found that the heat transfer coefficient decreased with the increase of salinity, the increase of salinity will cause the increase of liquid viscosity and decrease of surface disturbance, which will lead to the decrease of heat transfer coefficient. Fletcher et al. [12] carried out experimental research with seawater as working fluid, and found that the heat transfer coefficient of seawater is larger than that of water.

Liu et al. [13] studied the heat transfer performance of smooth horizontal tubes with outer diameters of $\phi13$, $\phi20$, and $\phi32$ mm, and observed that the heat transfer coefficient at the bottom of the horizontal tubes was slightly higher than at the top of the horizontal tubes. Rogers and Goindi [14] conducted an experiment using aluminum tubes of diameter $\phi132$ mm and discovered that in the thermal boundary development region, the experimental results of the heat transfer coefficient experiment were consistent with the results of theoretical calculations. Meanwhile, the measured values were lower than the theoretical values in the fully developed region. Kouhikamali et al. [15] found in an experiment that the heat transfer coefficient of the evaporator and the pressure drop across the tube bundles increased with the increase in temperature difference. While conducting a heat transfer experiment using R1234ze(E) and R24fa as working fluids, Jige et al. [16] discovered that at low heat flux density, convective heat transfer was the main factor that affected the heat transfer coefficient. In an experimental study on the effects of parameters, including spray density, heat flux, and evaporation temperature, on the convective heat transfer coefficient with water and seawater as working fluids, Mu et al. [17] found that the spray density had an effect on the heat transfer coefficient, but other parameters had less of an effect. Yang and Shen [18], who experimentally studied the effects of factors affecting heat transfer, such as liquid distributor height and heat flux, found that the heat transfer coefficient reached a maximum when using the optimal liquid distributor height. In an experimental study of the heat transfer performance of falling film evaporators using R134a as the working fluid, Ji et al. [19] discovered that the falling film flow rate had a significant effect on the heat transfer coefficient. Zheng et al. [20], who experimentally studied the evaporation heat transfer performance of tube materials with different surface wettability, observed that the use of superhydrophilic tubes could increase the heat transfer coefficient.

The parameters of horizontal-tube falling film evaporator under different working fluids have great influence on the heat transfer performance, and the heat transfer coefficient of the liquid film outside the horizontal tubes demonstrates a complex distribution. Current the experimental study of horizontal-tube falling film evaporator have mainly focused on the heat transfer performance in the entire area. Researches on the heat transfer performance of the crest and column of two important liquid films formed by the flow outside the liquid film tube are rarely involved. Additionally, relatively few controllable parameters have been studied owing to different research objectives and limitations of experiment. To improve the comprehensive heat transfer performance of horizontal tubes, this paper presents an experimental study using water and brine as working fluids. Then, the variation in the heat transfer coefficient of the crest and column sections outside a titanium-made heat exchanger tube are investigated by examining the flow rate, tube spacing, outer tube diameter, feed temperature, and salinity.

2. Experimental equipment and instruments

2.1. Experimental process

Fig. 1 illustrates the experimental process for a horizontal-tube falling film evaporator, while Fig. 2 depicts the equipment used in this experiment.

The experimental system includes the falling film process and the steam condensation process over the working fluid. The working fluid is first heated to the designated temperature in the working fluid tank before it is pumped to the upper tank. Under the action of gravity, the working fluid is controlled by the rotor flowmeter and then enters the evaporator. The stable liquid column formed through distribution by the spray tube is spread outside the test tube to realize the falling film flow process. Next, the electric heating rod installed in the test tube is turned on to heat the liquid film, which is then condensed by the condensate before it is recovered in the storage tank, thereby completing the steam condensation process. After the falling film flow process, the working fluid is collected in the recycling tank. This experiment was conducted under 54 KPa vacuum.

2.2. Experimental devices and measuring instruments

Three horizontal tubes are installed in the evaporator and are vertically arranged from top to bottom in the following order: spray tube, liquid distributor tube, and test tube. Fig. 3 depicts the falling film flow outside the horizontal tubes when the flow pattern of the liquid film between the tubes is a columnar flow. The outer diameter of the spray
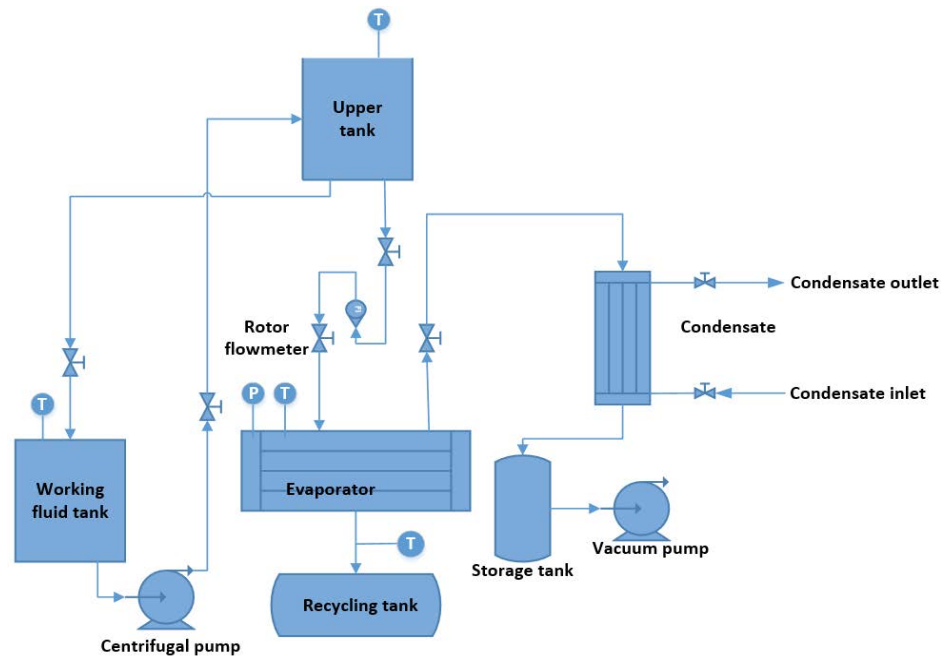
Fig. 1. Schematic diagram of experimental process.

Fig. 2. Experimental equipment.

Fig. 3. Falling film flow outside horizontal tubes.

at position $Z = 0$ mm represents the crest section, while the B–B section at position $Z = 30$ mm represents the column section.

Considering that the working fluid, that is, sodium chloride (NaCl) brine, is corrosive, the liquid distributor tube and the test tube are made of titanium. A titanium tube does not produce pitting in the brine and has excellent resistance to stress corrosion cracking. Additionally, a titanium tube has better hydrophilicity than a heat exchanger tube made of other materials, and can reduce the detachment of the liquid film at the tail of the heat exchanger tube from the tube wall, which is favorable to heat transfer in the liquid film.

A total of 10 measurement points are set on the outer wall of the test tube. Figs. 4 and 5 illustrate the configuration of the axial and circumferential measurement points, relatively. The axial measurement points are set along an

tube is 38 with 3 mm thickness; H is the distance between the spray tube and the liquid distributor tube, where $H = 8$ mm; λ is the center distance between two adjacent spray holes, where $\lambda = 20$ mm; d is the diameter of the spray hole, where $d = 2$ mm; D_1 is the outer diameter of the liquid distributor tube, where $D_1 = 25$ mm; D_2 is the outer diameter of the test tube, where $D_2 = 19, 25, 32,$ and 38 mm; and S is the distance between the outer diameter of the liquid distributor tube and the test tube, where $S = 5, 10,$ and 20 mm. Z is the axis direction of horizontal tube. The A–A section

axial distance of 30 mm. Considering that the test tube has a small diameter, the dense configuration of the circumferential measurement points will have an effect on the liquid film. Based on the symmetry of the round tube, the measurement points at positions 315° and 225° are used instead of the measurement points at positions 45° and 135°. A rectangular slot of dimensions 4 mm × 0.5 mm × 0.5 mm is opened at each measurement point to ensure that the measuring end of the sensor can be placed in the slot. The slot is also fixed with thermal conductive adhesives of high thermal conductivity. The temperature data
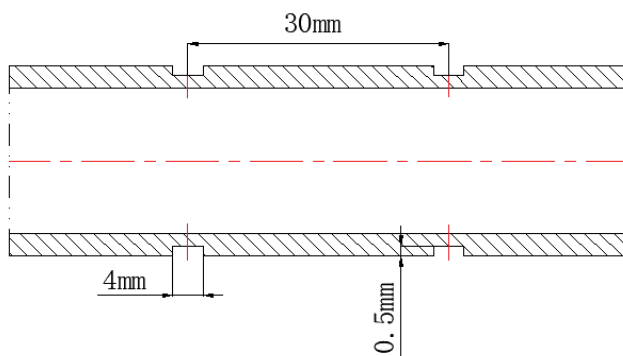
Fig. 4. Configuration of axial measurement points.
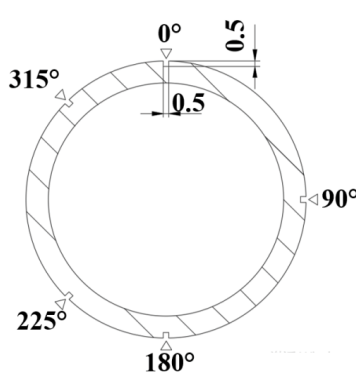
Fig. 5. Configuration of circumferential measurement points.

acquisition system, which consists of 16 temperature data channels, can simultaneously measure the temperature at 16 points. Temperature data are collected twice every second and automatically saved to a computer.

Table 1 presents a summary of the equipment and instruments used in this experiment.

3. Experimental data processing and error analysis

3.1. Experimental data processing

The experimental controllable parameters are the flow rate, tube spacing, outer tube diameter, fluid temperature, heat flux density, and salinity. The measurement parameter is the temperature at a measurement point on the outer wall of the test tube, which is used to calculate the local heat transfer coefficient. The experimental parameters are shown in Table 2.

During the experiment, the line of sight must be level with the rotor when the rotor flowmeter is reading data, and each group of flow data is read twice. After opening the slots on the test tube, its surface is smoothened with fine sandpaper so that the working fluid can freely fall off the outer surface of the tube. To reduce the heat loss in the working fluid during the experiment, the working fluid tank, evaporator, and related connecting tubes are equipped with insulating layers.

The heat flux density is controlled by the voltage regulator and is calculated using the following formula:

$$q_w = \frac{W}{A} = \frac{UI}{A} \tag{1}$$

The local heat transfer coefficient is calculated as follows:

$$h = \frac{q_w}{T - T_{sat}} = \frac{q_w}{\Delta T} \tag{2}$$

The salinity is defined as follows:

$$C = \frac{M_{salt}}{M_{salt} + M_{water}} \times 100\% \tag{3}$$

Table 1
Summary of experimental equipment and instruments

Name	Model	Measurement accuracy	Measuring range
Pressure sensor	HT-801-X	0.25% FS	−0.1–0 MPa
Vacuum gauge	YB150A	Level 0.4	−0.1–0 MPa
Thermocouple	Type-T	±0.2	−200°C–400°C
Temperature sensor	PT100	0.2%	−200°C–200°C
Temperature controller	XMTA-7411	0.1°C	0°C–300°C
Digital thermometer	Odatime KT300	0.1°C	−50°C–300°C
Rotor flowmeter	LZB-25F	1.5%	60–600 L/h
Voltage regulator	TDGC2J-3kVA	1%	0–250 V
Balance	Wante	0.01 g	0–3,000 g
Salinometer	DSM-25	±0.1%	0–28%

Table 2
Experimental parameters

Parameter	Range			
Flow rate, Q (L/h)	180	210	240	270
Tube spacing, S (mm)	5	10	20	
Outer tube diameter, D_2 (mm)	19	25	32	38
Fluid temperature, T (°C)	50	60	70	80
Heat flux density, q_w (W/m²)	12,000			
Salinity, C (%)	0	1	2	4

3.2. Experimental error analysis

Let the functional relationship between measured value Y and directly measurable parameters, $x_1, x_2, …, x_n$ be as follows:

$$Y = f(x_1, x_2, …, x_n) \tag{4}$$

The propagation of random errors is expressed as follows:

$$\frac{dY}{Y} = \left[\sum_{i=1}^{n}\left(\frac{\partial Y}{\partial x_i}\right)^2\right]^{\frac{1}{2}} \tag{5}$$

Based on the formula above, the error of the heat transfer coefficient obtained in this experiment is 5.13%.

4. Experimental results and analysis

4.1. Effect of flow rate

An experiment is conducted with D_1 = 25 mm, D_2 = 25 mm, and S = 10 mm. Water at 70°C is utilized as the working fluid. Adjusting Q = 180, 210, 240, and 270 L/h, and q_w = 12,000 W/m², to analyze the effect of flow rate on the local heat transfer coefficient.

To quantify the variation in the local heat transfer coefficient, the fluctuation range of the local heat transfer coefficient is defined in this study as follows:

$$\Delta h = \frac{h_{max}}{h_{min}} \times 100\% \tag{6}$$

Fig. 6a shows the effect of the flow rate on the local heat transfer coefficient of the crest section. According to this figure, the local heat transfer coefficient of the crest section increases with rising flow rate, but increases, decreases, and increases again with increasing circumferential angle. When Q = 270 L/h, the fluctuation range of its local heat transfer coefficient Δh is 1.693. Meanwhile, Δh is 1.458 when Q = 180 L/h. The local heat transfer coefficient reaches a maximum and minimum when θ = 45° and 135°, respectively. It is believed that the local heat transfer coefficient of the crest section is primarily affected by the thickness of the liquid film and fluid convergence. An increase in the thickness of the liquid film results in an increase in thermal resistance, which is not favorable to heat transfer, while fluid convergence is favorable to convective heat transfer. As the flow rate increases, the thickness of the liquid film in the crest section increases, and the converging liquid flow becomes stronger. Thus, its local heat transfer coefficient also rises owing to the greater effect of strong liquid convergence on the heat transfer.

Because the liquid film at θ = 0° and 45° in the crest section is located in the region with strong axial convergence, the local heat transfer coefficient of the crest section is higher. Meanwhile, the upper semi-circumference of the test tube at θ = 0° is located at the top of the tube, where the thickness of the liquid film reaches a maximum. In comparison, the thickness of the liquid film decreases at θ = 45°, so the local heat transfer coefficient at θ = 45° also decreases correspondingly. As the converging liquid flow becomes weaker at θ = 90° and 135°, its local heat transfer coefficient decreases correspondingly. At θ = 135°, the local heat transfer coefficient reaches a minimum. Meanwhile, the local heat transfer coefficient increases significantly owing to the circumferential convergence of the fluid at θ = 180°.
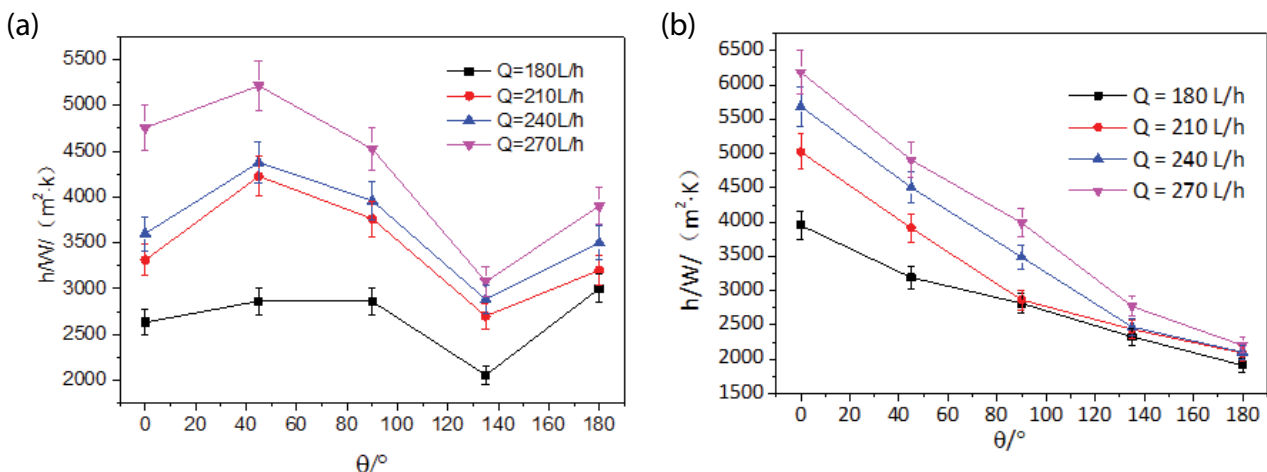
Fig. 6. Effect of flow rate on local heat transfer coefficient of (a) crest and (b) column section.

Fig. 6b displays the effect of the flow rate on the local heat transfer coefficient of the column section. According to Fig. 6, its local heat transfer coefficient increases with a rising flow rate and decreases with an increasing circumferential angle. The local heat transfer coefficient fluctuates within a range of Δh = [2.066, 2.807], and Δh reaches a maximum when Q = 270 L/h. It is believed that the local heat transfer coefficient of the column section is primarily affected by the thickness of the liquid film and fluid impingement. With the increase of flow rate, the impact effect of fluid is enhanced, which is beneficial to convective heat transfer, so the local heat transfer coefficient increases.

Because the liquid film at θ = 0° in the column section is located in the direct fluid impingement region, this region experiences maximum fluid impingement, so its local heat transfer coefficient reaches a maximum. As the impingement effect decreases at θ = [45°, 90°, 135°, and 180°] with increasing distance from the liquid column impingement region, the distribution of the local heat transfer coefficient gradually decreases along the circumferential direction.

4.2. Effect of tube spacing

An experiment is conducted with D_1 = 25 mm, D_2 = 25 mm, and S = 5, 10, and 20 mm. Water at 70°C is utilized as the working fluid. Controlling Q = 210 L/h and q_w = 12,000 W/m², to analyze the effect of tube spacing on the local heat transfer coefficient.

Fig. 7a displays the effect of the tube spacing on the local heat transfer coefficient of the crest section. According to Fig. 7, the local heat transfer coefficient of the crest section decreases with rising tube spacing. Its local heat transfer coefficient fluctuates within a range of Δh = [1.361, 1.433] and reaches a maximum and minimum at θ = 45° and 135°, respectively. With the increase of tube spacing, the impact effect of liquid column formed by distribution pipe is enhanced. This results in the accumulation of fluid along the test tube when axial convergence occurs, thereby leading to the enlargement of the liquid film in the crest section. Hence, the local heat transfer coefficient decreases. The variation trend of local heat transfer coefficient with circumferential angle is consistent with Fig. 6a.

Fig. 7b shows the effect of the tube spacing on the local heat transfer coefficient of the column section. According to this figure, the local heat transfer coefficient of the column section rises with increasing tube spacing. Its local heat transfer coefficient fluctuates within a range of Δh = [2.099, 2.403] and reaches a maximum when S = 20 mm. It is believed that with an increase in the tube spacing, the impingement effect on the liquid flowing from the liquid column in the liquid distributor tube to the top of the test tube increases. This increases the flow of the liquid film, thereby causing an increase in the local heat transfer coefficient. With the same tube spacing, the fluid impingement effect on the positions of measurement points at θ = [45°, 90°, 135°, and 180°] in the column section becomes weaker, so its local heat transfer coefficient decreases.

4.3. Effect of outer tube diameter

An experiment is conducted with D_1 = 25 mm, D_2 = 19, 25, 32, and 38 mm, and S = 10 mm. Water at 70°C is utilized as the working fluid. Controlling Q = 210 L/h and q_w = 12,000 W/m², to analyze the effect of outer tube diameter on the local heat transfer coefficient.

Fig. 8a shows the effect of the outer tube diameter on the local heat transfer coefficient of the crest section. At θ = 0° to 45°, the local heat transfer coefficient increases with an increasing outer tube diameter. At θ = 90°–180°, the local heat transfer coefficient of the tubes with D_2 = 25, 32, and 38 mm decreases with an increasing outer tube diameter, while variations in the local heat transfer coefficient of the tube with D_2 = 19 mm are inconsistent with those of other horizontal tubes. The local heat transfer coefficient of the crest section fluctuates within a range of Δh = [1.354, 1.821], and Δh reaches a maximum when D_2 = 38 mm. The curvature of the arc at the top of the tube decreases when the outer diameter of the tube increases, and the liquid film with θ = 0°–45° on the top of the test tube is easier to spread along the axial direction, and more liquid converges at the crest section, therefore, the local heat transfer coefficient is higher at θ = 45°. At θ = 90°–180°, with the increase of spreading area of liquid in the lower half circle of D_2 = 25, 32, and 38 mm, the higher the energy loss of these
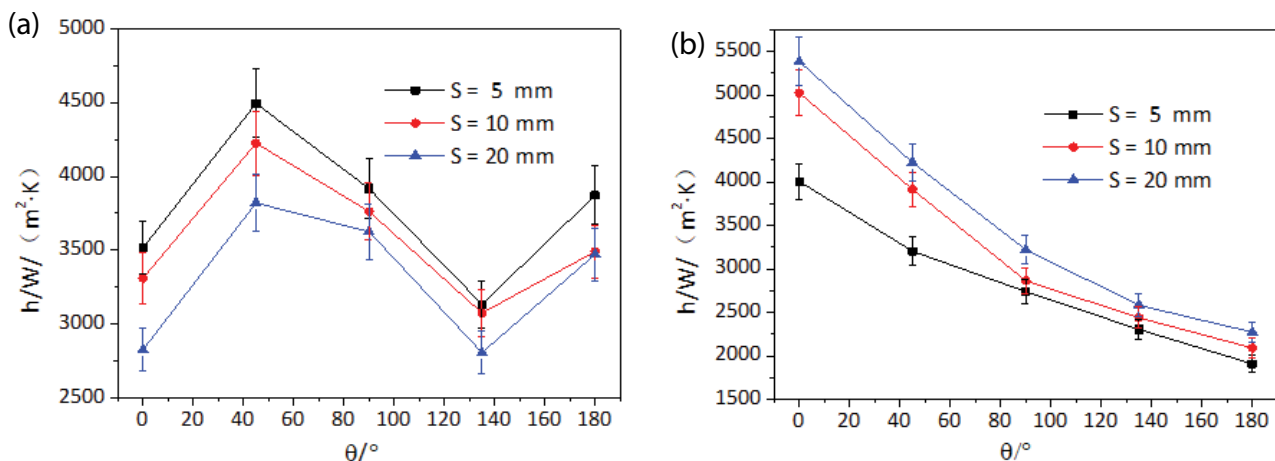
Fig. 7. Effect of tube spacing on local heat transfer coefficient of (a) crest and (b) column section.

tubes, and the convergence effect of liquid film becomes weaker, thereby resulting in a decrease in the local heat transfer coefficient with an increasing outer tube diameter.

When D_2 = 19 mm, because the outer diameter of test tube D_2 is smaller than the outer diameter of distribution pipe D_1, the kinetic energy of liquid film flow in the lower half circle of test tube increases, but the thickness of liquid film also increases. Due to the comprehensive effect of these two factors, the local heat transfer coefficient of D_2 = 19 mm is between D_2 = 25 and 32 mm, and its circumferential average local heat transfer coefficient is smaller than that of other horizontal tubes.

Fig. 8b depicts the effect of the outer tube diameter on the local heat transfer coefficient of the column section. At θ = 0°, the local heat transfer coefficient rises with an increasing outer tube diameter. At θ = 45°–180°, the local heat transfer coefficient decreases with an increasing outer tube diameter. The local heat transfer coefficient of the column section fluctuates within a range of Δh = [2.035, 3.083], and Δh reaches a maximum when D_2 = 38 mm. It is believed that with the same outer tube diameter, the local heat transfer coefficient of the column section decreases from θ = 0° to 180° because the fluid impingement effect at the position of each measurement point in the circumferential direction becomes weaker. In addition, at θ = 0°, the fluid impingement effect on the liquid film increases with an increasing outer tube diameter, resulting in an increase in the local heat transfer coefficient. At θ = 45°–180°, the variation range of kinetic energy of the liquid film flow decreases as the outer tube diameter increases, leading to a decrease in the local heat transfer coefficient.

4.4. Effect of feed temperature

An experiment is conducted with D_1 = 25 mm, D_2 = 25 mm, and S = 10 mm. Water at 50°C, 60°C, 70°C, and 80°C are utilized as the working fluid. Controlling Q = 210 L/h and q_w = 12,000 W/m², to analyze the effect of feed temperature on the local heat transfer coefficient.

Figs. 9a and b show the effect of the feed temperature on the local heat transfer coefficient of the crest section and

the column section. According to these figures, the local heat transfer coefficients of the crest and column sections increase as the feed temperature rises. The crest section is local heat transfer coefficient fluctuates within a range of Δh = [1.368, 1.565] and reaches a maximum at T = 80°C. On the other hand, the column section is local heat transfer coefficient fluctuates within a range of Δh = [2.177, 2.650] and reaches a maximum at T = 80°C.

It is believed that the physical properties of water are greatly affected by the temperature, and the viscosity and surface tension of water decrease with rising temperature. A decrease in viscosity results in a decrease in the spreading resistance of the fluid, an increase in the flow velocity of the fluid, and a decrease in the thickness of the liquid film. A decrease in the surface tension causes the restraining force of the spreading liquid film to become weaker and the flow of the liquid film to become stronger, leading to an increase in the local heat transfer coefficient. As axial convergence is present in the liquid film at θ = 0° and 45° and circumferential convergence is present in the liquid film at θ = 180° in the crest section, the variation in its local heat transfer coefficient with the circumferential angle is consistent with that shown by the curves in Fig. 6a. Meanwhile, as the liquid column impingement effect is present at θ = 0° in the column section at the top of the test tube while the impingement effect occurs at other positions, that is, θ = [45°, 90°, 135°, and 180°] gradually decreases, the distribution of the local heat transfer coefficient decreases along the circumferential direction.

4.5. Effect of salinity

An experiment is conducted with D_1 = 25 mm, D_2 = 25 mm, and S = 10 mm. Brine at 60°C is utilized as the working fluid. Adjusting C = 0%, 1%, 2%, and 4%, Q = 210 L/h, and q_w = 12,000 W/m², to analyze the effect of salinity on the local heat transfer coefficient.

Figs. 10a and b show the effect of salinity on the local heat transfer coefficient of the crest section and column section. According to Fig. 10, the local heat transfer coefficients of the crest and column sections decrease with increasing
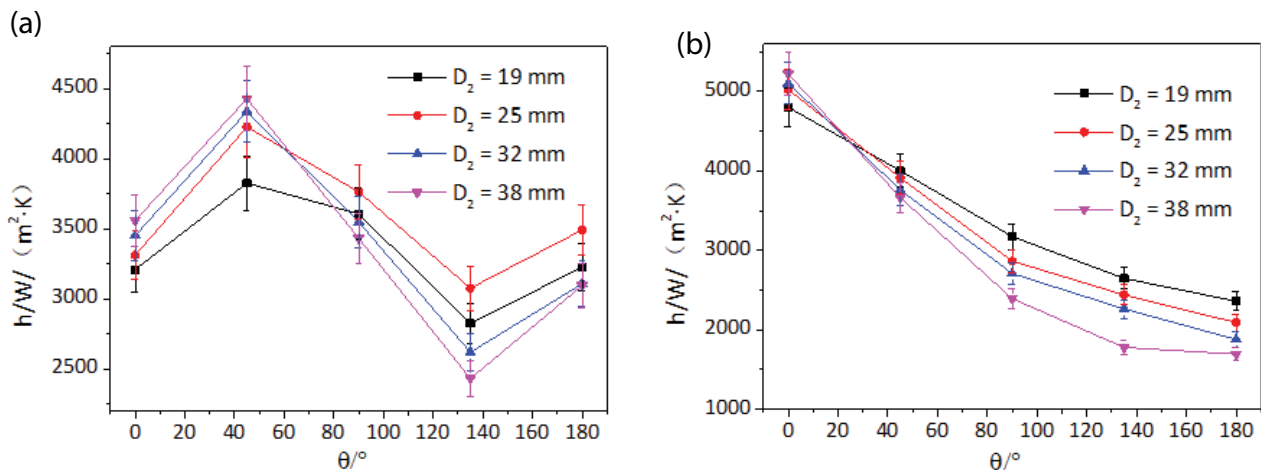
Fig. 8. Effect of outer tube diameter on local heat transfer coefficient of (a) crest and (b) column section.
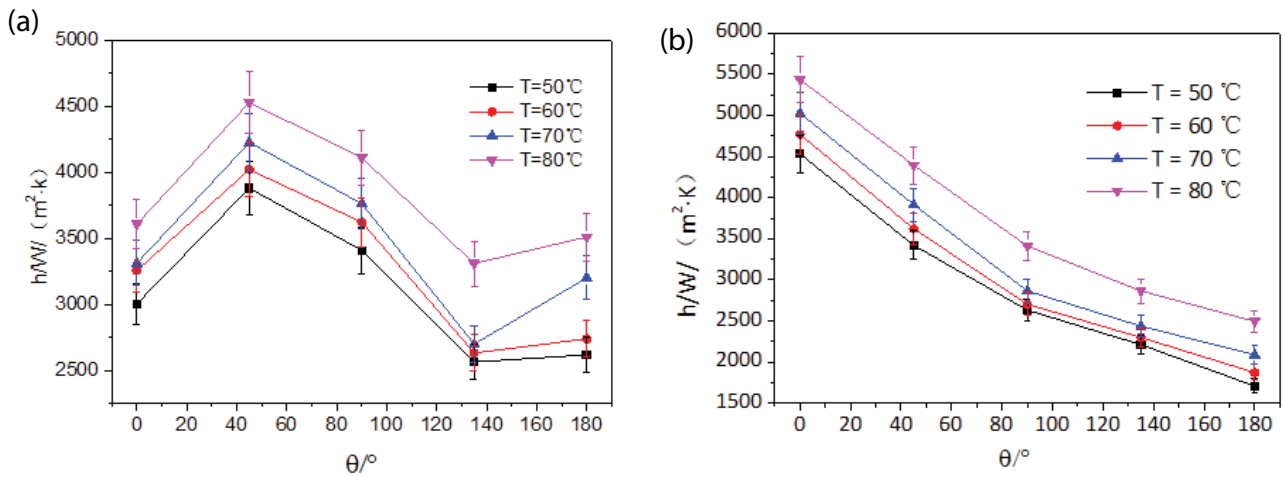
Fig. 9. Effect of feed temperature on local heat transfer coefficient of (a) crest and (b) column section.
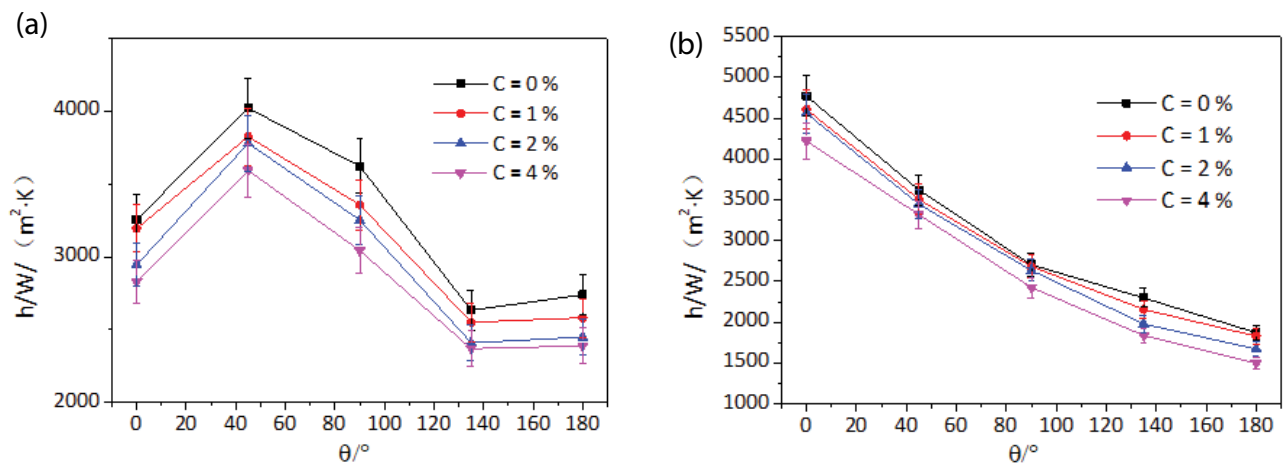
Fig. 10. Effect of salinity on local heat transfer coefficient of (a) crest and (b) column section.

salinity. The crest section is local heat transfer coefficient fluctuates within a range of $\Delta h = [1.499, 1.568]$ and reaches a minimum when $C = 4\%$. Meanwhile, the column section is local heat transfer coefficient fluctuates within a range of $\Delta h = [2.517, 2.812]$ and reaches a minimum when $C = 4\%$.

It is believed that as the salinity increases, the viscosity and surface tension of the brine increase. Furthermore, an increase in viscosity results in an increase in the thickness of the brine liquid film, while an increase in the surface tension causes the flow of the liquid film to be weaker. These two factors are not favorable to heat transfer, leading to a decrease in the local heat transfer coefficient. Based on the analysis above, as different axial and circumferential convergence regions are present in the liquid film, the variation in the local heat transfer coefficient with the circumferential angle is consistent with that shown by the curves in Figs. 6a, 7a, and 9a. Owing to the different strengths of the liquid column impingement effect at the circumferential positions of the test tube, the distribution of the local heat transfer coefficient of the column section decreases along the circumferential direction.

4.6. Comparisons with other work

The average values of the crest and column section in this paper are compared with experimental values of Xu [17]. The results show that the effect of flow rate on local heat transfer coefficient is the same as that of Xu's spray density, and the change trend of local heat transfer coefficient with circumferential angle is consistent. The comparison results are shown in Fig. 11.

5. Fitting equation of local heat transfer coefficient

From the above experimental analysis, the flow rate, feed temperature, salinity, and other factors can affect the heat transfer performance of falling film evaporation outside the tube. According to the experimental data obtained, the local heat transfer coefficients of the crest and column section are fitted, respectively.

The fitting equation of the crest section is as follows:

$$Nu = 9.022 \times 10^{-5} \times Re^{0.973}Pr^{1.177} \tag{7}$$
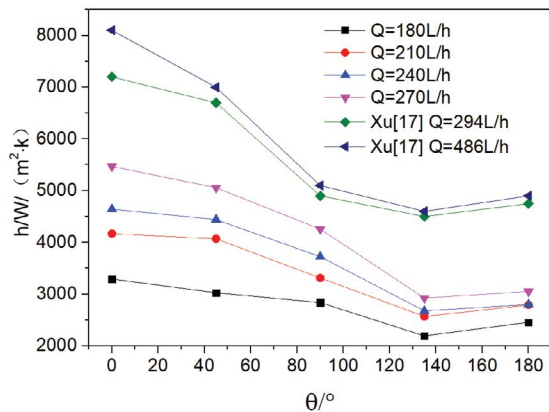
Fig. 11. Comparison with previous studies.

The correlation coefficient of fitting equation of the crest section is adjusted R^2 = 0.852. The relative error between the experimental value and the calculated value is within ±9%.

The fitting equation of the column section is as follows:

$$\text{Nu} = 2.685 \times 10^{-4} \times \text{Re}^{0.836}\text{Pr}^{0.918} \tag{8}$$

The correlation coefficient of fitting equation of the column section is adjusted R^2 = 0.893. The relative error between the experimental value and the calculated value is within ±7%.

6. Conclusions

The crest and column are the important areas of liquid film flow. In this paper, the effect of the flow rate, tube spacing, outer tube diameter, feed temperature, and salinity on the local heat transfer coefficient outside titanium-made horizontal tubes were analyzed by using water and brine (with salinity C = 1%, 2%, and 4%) as the working fluids. The following conclusions were drawn:

- An experiment was conducted with Q = 180, 210, 240, and 270 L/h to study the effect of flow rate on the local heat transfer coefficient. The results indicate that the local heat transfer of the crest section is primarily affected by the thickness of the liquid film and fluid convergence, the local heat transfer coefficient of the crest section increases with rising flow rate. However, with increase in circumferential angle, the local heat transfer coefficient increases, decreases, and again increases. The local heat transfer coefficient fluctuates within a range of Δh = [1.378, 1.693]. It reaches the maximum at θ = 45°, and reaches the minimum at θ = 135°. Meanwhile, the local heat transfer coefficient of the column section is mainly affected by the thickness of the liquid film and fluid impingement, where its local heat transfer coefficient increases with an increasing flow rate but decreases with an increasing circumferential angle. The local heat transfer coefficient fluctuates within a range of Δh = [2.066, 2.807], and Δh reaches a maximum when Q = 270 L/h.

- An experiment was conducted using S = 5, 10, and 20 mm to investigate the effect of tube spacing on the local heat transfer coefficient. According to the experimental results, the local heat transfer coefficient of the crest section decreases with increasing tube spacing. The local heat transfer coefficient fluctuates within a range of Δh = [1.361, 1.433]. It reaches the maximum at θ = 45°, and reaches the minimum at θ = 135°. On the other hand, the local heat transfer coefficient of the column section increases with an increasing tube spacing. The local heat transfer coefficient fluctuates within a range of Δh = [2.099, 2.403] and reaches a maximum when S = 20 mm.

- An experiment was conducted using D_2 = 19, 25, 32, and 38 mm to study the effect of the outer tube diameter on the local heat transfer coefficient. According to the results of this experiment, at θ = 0°–45°, the local heat transfer coefficient of the crest section increases with an increasing outer tube diameter. At θ = 90°–180°, the local heat transfer coefficient of the tube with D_2 = 19 mm lies between that of the tubes with D_2 = 25 and 32 mm. However, the local heat transfer coefficient of the tubes with D_2 = 25, 32, and 38 mm decrease with an increasing outer tube diameter. The local heat transfer coefficient of the crest section fluctuates within a range of Δh = [1.354, 1.821], and Δh reaches a maximum when D_2 = 38 mm.

On the other hand, at θ = 0°, its local heat transfer coefficient of the column section increases with an increasing outer tube diameter. At θ = 45°–180°, the local heat transfer coefficient decreases with an increasing outer tube diameter. The local heat transfer coefficient of the column section fluctuates within a range of Δh = [2.035, 3.083], and Δh reaches a maximum when D_2 = 38 mm.

- An experiment was conducted with water (T = 50°C, 60°C, 70°C, and 80°C) as the working fluid to investigate the effect of feed temperature on the local heat transfer coefficient. It is found that the local heat transfer coefficients of the crest and column sections increase with an increasing feed temperature. The crest section is local heat transfer coefficient fluctuates within a range of Δh = [1.368, 1.565]. It reaches a maximum at T = 80°C. On the other hand, the column section is local heat transfer coefficient fluctuates within a range of Δh = [2.177, 2.650] and reaches a maximum at T = 80°C.

- An experiment was conducted with brine (salinity C = 0%, 1%, 2%, and 4%) to study the effect of salinity on the local heat transfer coefficient. The results show that the local heat transfer coefficients of the crest and column sections decrease with increasing salinity. The local heat transfer coefficient at crest section fluctuates within a range of Δh = [1.499, 1.568] and reaches a minimum when C = 4%. Meanwhile, the local heat transfer coefficient at column section fluctuates within a range of Δh = [2.517, 2.812] and reaches a minimum when C = 4%.

Symbols

A	—	External surface area of heat exchange tube, m²
C	—	Salinity, %

d	—	Spray hole diameter, mm
D_1	—	External diameter of liquid distributor tube, mm
D_2	—	External diameter of test tube, mm
h	—	Local heat transfer coefficient, W/(m² K)
H	—	Spray height, mm
h_{max}	—	Maximum value of local heat transfer coefficient, W/(m² K)
h_{min}	—	Minimum value of local heat transfer coefficient, W/(m² K)
I	—	Input current of heating rod, A
M	—	Mass, kg
Nu	—	Nusselt number
Pr	—	Planck number
q_w	—	Heat flux, W/m²
Re	—	Reynolds number
S	—	Tube spacing, mm
T	—	Temperature, °C
T_{sat}	—	Saturated evaporation temperature, °C
U	—	Input voltage of heating rod, V
Γ	—	Spray density, kg/m s
Δh	—	Fluctuation amplitude of local heat transfer coefficient

Greek

λ	—	Adjacent spray hole distance, mm
θ	—	Circumferential angle, °
δ	—	Liquid film thickness, mm

References

[1] I.S. Al-Mutaz, Features of multi-effect evaporation desalination plants, Desal. Water Treat., 54 (2015) 3227–3235.
[2] F. Wunder, S. Enders, R. Semiat, Numerical simulation of heat transfer in a horizontal falling film evaporator of multiple-effect distillation, Desalination, 401 (2017) 206–229.
[3] S. Bajalan, R. Kouhikamali, M.H. Rahimian, Experience on horizontal-tube falling-film evaporation simulation by lattice-Boltzmann method, Heat Transfer Asian Res., 48 (2019) 2676–2699.
[4] H. Hou, Q. Bi, X. Zhang, Numerical simulation and performance analysis of horizontal-tube falling-film evaporators in seawater desalination, Int. Commun. Heat Mass Transfer, 39 (2012) 46–51.
[5] Q. Qiu, X. Zhang, S. Quan, X. Zhu, S. Shen, 3D numerical study of the liquid film distribution on the surface of a horizontal-tube falling-film evaporator, Int. J. Heat Mass Transfer, 124 (2018) 943–952.
[6] W.H. Parken, L.S. Fletcher, V. Sernas, J.C. Han, Heat transfer through falling film evaporation and boiling on horizontal tubes, J. Heat Transfer, 112 (1990) 744–750.
[7] E.N. Ganic, M.N. Roppo, An experimental study of falling liquid film breakdown on a horizontal cylinder during heat transfer, J. Heat Transfer, 102 (1980) 342–346.
[8] X. Hu, A.M. Jacobi, The intertube falling film: part 2 – mode effects on sensible heat transfer to a falling liquid film, J. Heat Transfer, 118 (1996) 626–633.
[9] L. Xu, M. Ge, S. Wang, Y. Wang, Heat-transfer film coefficients of falling film horizontal tube evaporators, Desalination, 166 (2004) 223–230.
[10] V.N. Slesarenko, Thermal desalination of sea water in thin film-plants, Desalination, 45 (1983) 295–302.
[11] V.N. Slesarenko, Investigation of heat exchange during sea water boiling in a horizontal thin film desalination plant, Desalination, 29 (1979) 311–318.
[12] L.S. Fletcher, V. Sernas, W.H. Parken, Evaporation heat transfer coefficients for thin sea water films on horizontal tubes, Ind. Eng. Chem. Process Des. Dev., 14 (1975) 411–416.
[13] Z. Liu, Q. Zhu, Y. Chen, Evaporation heat transfer of falling water film on a horizontal tube bundle, Heat Transfer Asian Res., 31 (2002) 42–55.
[14] J.T. Rogers, S.S. Goindi, Experimental laminar falling film heat transfer coefficients on a large diameter horizontal tube, Can. J. Chem. Eng., 67 (1989) 560–568.
[15] R. Kouhikamali, S.M.A. Noori Rahim Abadi, M. Hassani, Numerical investigation of falling film evaporation of multi-effect desalination plant, Appl. Therm. Eng., 70 (2014) 477–485.
[16] D. Jige, H. Miyata, N. Inoue, Falling film evaporation of R1234ze(E) and R245fa on a horizontal smooth tube, Exp. Therm. Fluid Sci., 105 (2019) 58–66.
[17] X. Mu, S. Shen, Y. Yang, X. Liu, Experimental study of falling film heat transfer coefficient on horizontal tube, Desal. Water Treat., 50 (2012) 310–316.
[18] L. Yang, S. Shen, Experimental study of falling film evaporation heat transfer outside horizontal tubes, Desalination, 220 (2008) 654–660.
[19] W. Ji, C. Zhao, D. Zhang, S. Yoshioka, Y. He, W. Tao, Effect of vapor flow on the falling film evaporation of R134a outside a horizontal tube bundle, Int. J. Heat Mass Transfer, 92 (2016) 1171–1181.
[20] Y. Zheng, X. Ma, Y. Li, R. Jiang, K. Wang, Z. Lan, Q. Liang, Experimental study of falling film evaporation heat transfer on superhydrophilic horizontal-tubes at low spray density, Appl. Therm. Eng., 111 (2017) 1548–1556.